

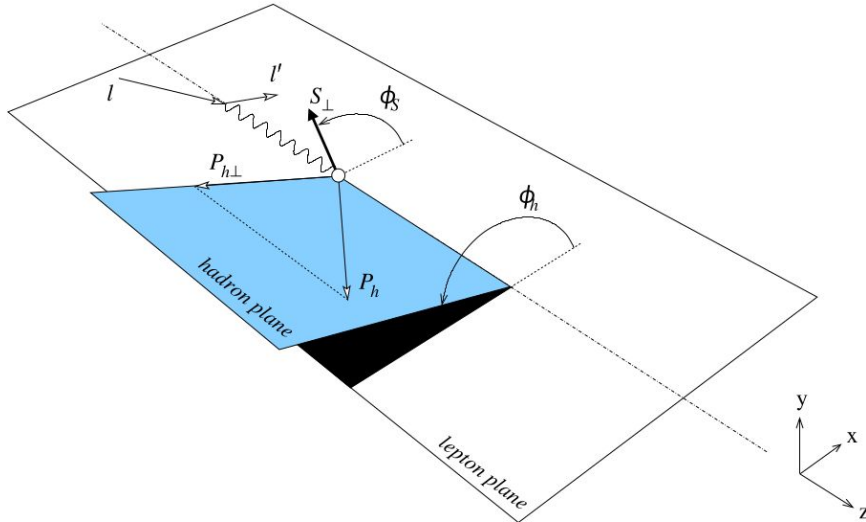
# High momentum kaon Beam-Spin Asymmetry

Simone Vallarino  
INFN Genova  
November 13, 2024

# Semi-Inclusive DIS

SIDIS is the scattering of a lepton over a nucleon, producing a final state on which the scattered lepton and at least one hadron are detected.

$$\ell(l) + N(P) \rightarrow \ell(l') + h(P_h) + X$$

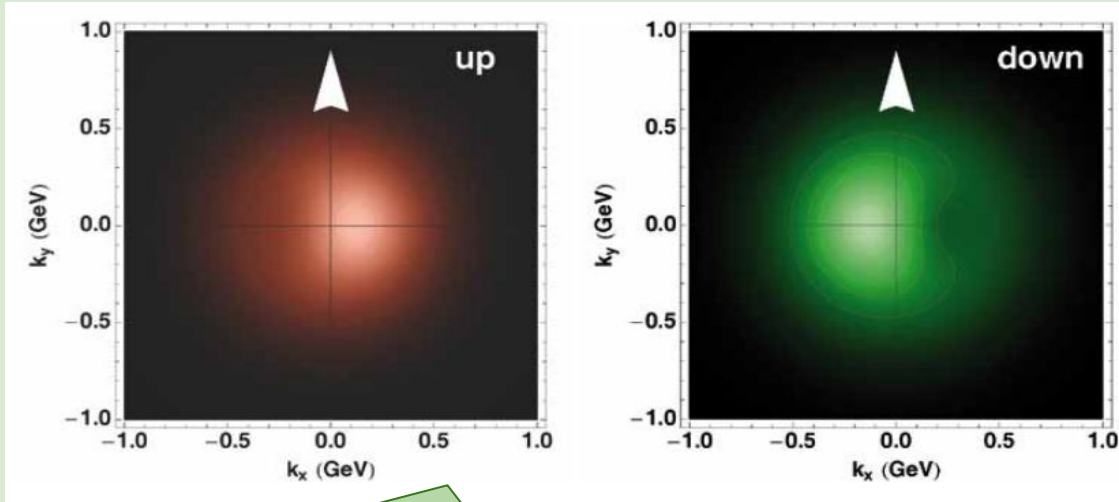


$$\frac{d\sigma}{dx dy d\psi dz d\phi_h dP_{h\perp}^2} = \begin{matrix} \nearrow \\ \text{F}_{\text{beam, target, virtual photon}} \\ \text{polarization} \end{matrix} \left\{ \begin{aligned} & F_{UU,T} + \varepsilon F_{UU,L} + \sqrt{2\varepsilon(1+\varepsilon)} \cos\phi_h F_{UU}^{\cos\phi_h} \\ & + \varepsilon \cos(2\phi_h) F_{UU}^{\cos 2\phi_h} + \lambda_e \sqrt{2\varepsilon(1-\varepsilon)} \sin\phi_h F_{LU}^{\sin\phi_h} \\ & + S_{\parallel} \left[ \sqrt{2\varepsilon(1+\varepsilon)} \sin\phi_h F_{UL}^{\sin\phi_h} + \varepsilon \sin(2\phi_h) F_{UL}^{\sin 2\phi_h} \right] \\ & + S_{\parallel} \lambda_e \left[ \sqrt{1-\varepsilon^2} F_{LL} + \sqrt{2\varepsilon(1-\varepsilon)} \cos\phi_h F_{LL}^{\cos\phi_h} \right] \\ & + |S_{\perp}| \left[ \sin(\phi_h - \phi_S) \left( F_{UT,T}^{\sin(\phi_h - \phi_S)} + \varepsilon F_{UT,L}^{\sin(\phi_h - \phi_S)} \right) \right. \\ & \quad + \varepsilon \sin(\phi_h + \phi_S) F_{UT}^{\sin(\phi_h + \phi_S)} + \varepsilon \sin(3\phi_h - \phi_S) F_{UT}^{\sin(3\phi_h - \phi_S)} \\ & \quad \left. + \sqrt{2\varepsilon(1+\varepsilon)} \sin\phi_S F_{UT}^{\sin\phi_S} + \sqrt{2\varepsilon(1+\varepsilon)} \sin(2\phi_h - \phi_S) F_{UT}^{\sin(2\phi_h - \phi_S)} \right] \\ & + |S_{\perp}| \lambda_e \left[ \sqrt{1-\varepsilon^2} \cos(\phi_h - \phi_S) F_{LT}^{\cos(\phi_h - \phi_S)} + \sqrt{2\varepsilon(1-\varepsilon)} \cos\phi_S F_{LT}^{\cos\phi_S} \right. \\ & \quad \left. + \sqrt{2\varepsilon(1-\varepsilon)} \cos(2\phi_h - \phi_S) F_{LT}^{\cos(2\phi_h - \phi_S)} \right] \end{aligned} \right\}$$

# Polarized SIDIS to investigate the 3D nucleon structure

Measuring the structure function  $F_{LU}$  can provide access to Transverse-Momentum Dependent Parton Distribution Functions.

$$F_{LU}^{\sin\phi} = \frac{2M}{Q} \mathcal{C} \left[ \frac{\hat{\mathbf{h}} \cdot \mathbf{k}_T}{M_H} \left( x_B e H_1^\perp + \frac{M_h}{M} f_1 \frac{\tilde{G}^\perp}{z} \right) + \frac{\hat{\mathbf{h}} \cdot \mathbf{p}_T}{M} \left( x_B g^\perp D_1 + \frac{M_h}{M} h_1^\perp \frac{\tilde{E}}{z} \right) \right]$$



Up and down momentum distribution inside a polarized nucleon.

Strange quark:



That's why we need to study kaon SIDIS!

# Measuring the structure function: Beam-Spin Asymmetry

$$\lambda_e \sqrt{2\varepsilon(1-\varepsilon)} \sin \phi_h F_{LU}^{\sin \phi_h}$$

$\phi^h \rightarrow \phi$

Definition of the Beam-Spin Asymmetry generated by the longitudinal polarization of beam

$$A_{LU} = \frac{d\sigma^+ - d\sigma^-}{d\sigma^+ + d\sigma^-} = \frac{A_{LU}^{\sin \phi^h} \sin \phi^h}{1 + A_{UU}^{\cos \phi^h} \cos \phi^h + A_{UU}^{\cos 2\phi^h} \cos 2\phi^h}$$

Experimental definition of BSA

$$A_{LU}(\phi) = \frac{1}{P_b} \frac{N^+ - N^-}{N^+ + N^-}$$

$N^\pm$  indicates the number of events for beam with  $\pm$  helicity;  
 $P_b$  is the beam polarization

$$A_{LU}^{\sin \phi} = \frac{\sqrt{2\varepsilon(1-\varepsilon)} F_{LU}^{\sin \phi}}{F_{UU}}$$

Relation between asymmetry term and structure-function

# Unbinned Maximum Likelihood method

The UML method removes the binning systematic effects but is more expensive in terms of computation. It was evaluated as more convenient for this kind of study.

$$PDF(x_i, \alpha) = \frac{\sigma_{UU}(1 + A_i(\alpha))}{\mathcal{N}(\int d\sigma_{UU})}$$

$d\sigma$  does not depend from  $\alpha$

$$PDF(x_i, \alpha) = 1 + A_i(\alpha)$$

$$\mathcal{L} = \prod_{i=1}^N PDF(x_i, \alpha)$$

Likelihood definition

$$\log \mathcal{L} = \sum_i^N \log [PDF(x_i, \alpha)]$$

$$\chi^2 = -2 \log \mathcal{L}$$

If large sample of independent measurement

PDF for Beam Spin Asymmetry

Beam polarization

$$PDF_{\pm}(x_i, A_{LU}^{\sin \phi}) = 1 \pm P_b(A_{LU}^{\sin \phi} \sin \phi_i)$$

Relation between structure-function and asymmetry

$$A_{LU}^{\sin \phi} = \frac{\sqrt{2\varepsilon(1-\varepsilon)}F_{LU}^{\sin \phi}}{F_{UU}}$$

$$\log \mathcal{L} = \sum_i^{N^++N^-} \log \left[ 1 \pm P_b \left( \frac{\sqrt{2\varepsilon(1-\varepsilon)}F_{LU}^{\sin \phi}}{F_{UU}} \sin \phi_i \right) \right]$$

Function to minimize

# Analysis

# Analysis procedure

To study  $eK^+X$  BSA using RG-A data and cross-check the results obtained by [M. Mirazita](#).

→ Currently ongoing. Some difficulties emerged in achieving the same statistical precision; I'm investigating the causes.

To apply the analysis on RG-B data and extract the first kaon BSA using deuterium at CLAS12.

→ Currently started. The implementation of the new pass2 fiducial cut is ongoing. I can show the first preliminary BSA plots for RG-B kaon SIDIS.

To compare the results with the simulation and provide feedback to our theory experts.

→ Next step. H. Avagyan produced simulated data for proton and neutron targets, I will use this material to compare

# Data selection criteria

Final state:  $eK^+ X$

Electron selection criteria:

- electron in the forward detector;
- vertex z included in (-8,3) cm for inbending and (-10,2.5) cm for outbending;
- HTCC number of photons  $> 2$ ;
- PCAL energy  $> 0.07$  GeV;
- pass1 calorimeter sampling and fiducial cut by T. Hayward (need to check for pass2);
- track edge for DC 1  $> 5$ , for DC2  $> 5$ , for DC3  $> 10$  (preliminary cuts got from T. Hayward fiducial cuts for RG-C);
- track  $\chi^2 < 80$ .

Kaon selection criteria:

- kaon identified by the RICH;
- vertex z included in (-10,2.5) cm for inbending and (-8,3) cm for outbending;
- track edge for DC 1  $> 3$ , for DC2  $> 3$ , for DC3  $> 7$  (preliminary cuts got from T. Hayward fiducial cuts for RG-C);
- track  $\chi^2 < 80$ ;
- RICH number of photoelectrons  $> 2$ ;
- RICH RQ  $> 0.1$ .

Several selection criteria are going to be updated with new pass2 fiducial cuts presented by T. Hayward in Oct 16th.

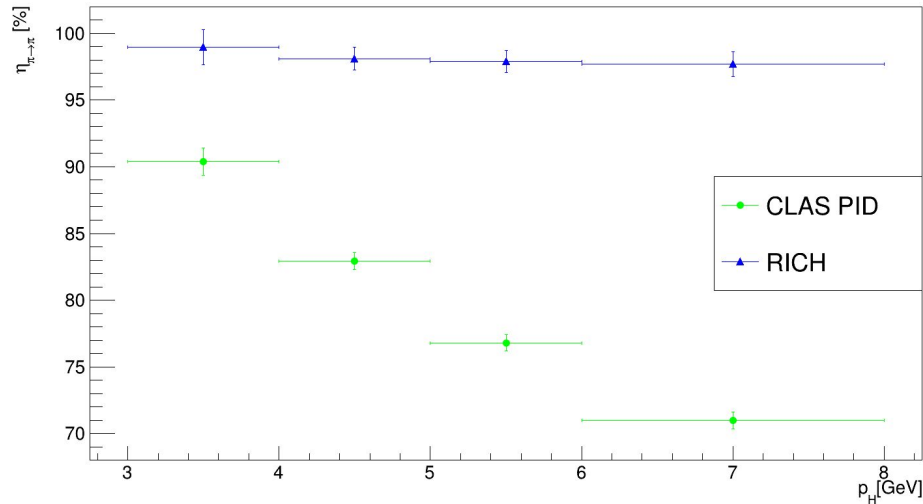
$$RQ = 1 - \frac{\lambda_{best}}{\lambda_{second\_best}}$$



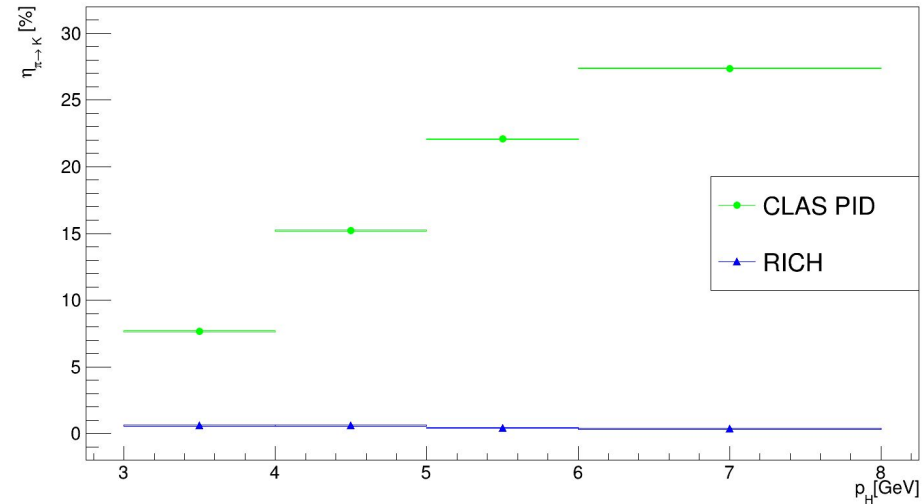
# Why the RICH

I'm specifically using kaon identified by the RICH because it is the only detector capable to efficiently identify them in the 3-8 GeV/c momentum range.

Pion correctly identified



Pion misidentified as a kaon



# Kinematical cuts and data samples analyzed.

Kinematical cuts are the SIDIS typical selection criteria:

- $Q^2 > 1.0 \text{ GeV}^2$ ;
- $W > 2.0 \text{ GeV}$ ;
- $x_F > 0.0$ ;
- $y < 0.75$ ;
- $MM > 1.6 \text{ GeV}$ .

Combined with particle selection criteria

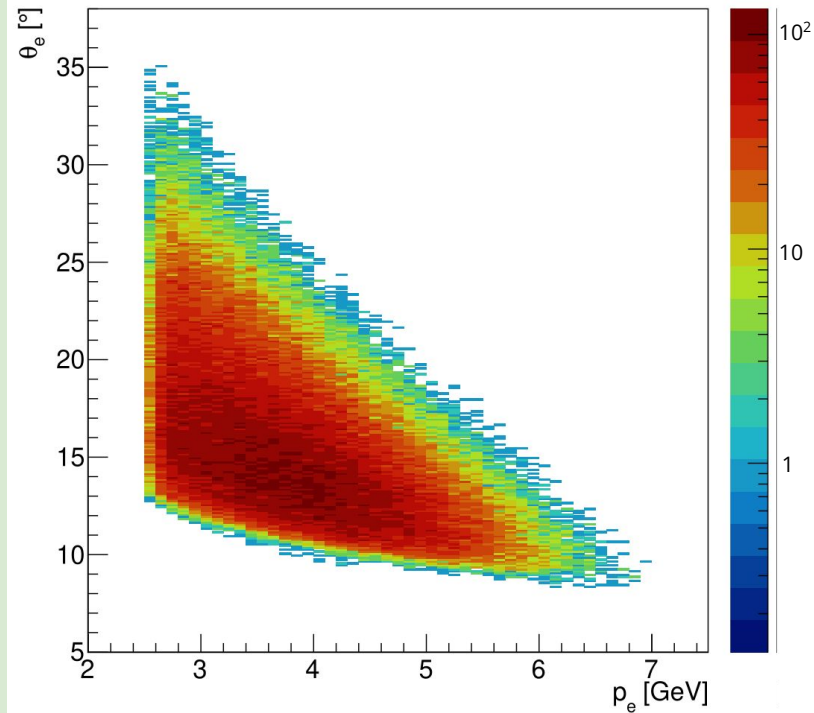
Analysis on going:

- RG-A inbending data (fall18 and spring 19);
- RG-A outbending data (fall18);
- RG-B full sample (spring19, fall 19 and spring 20).

# Phase space - electron

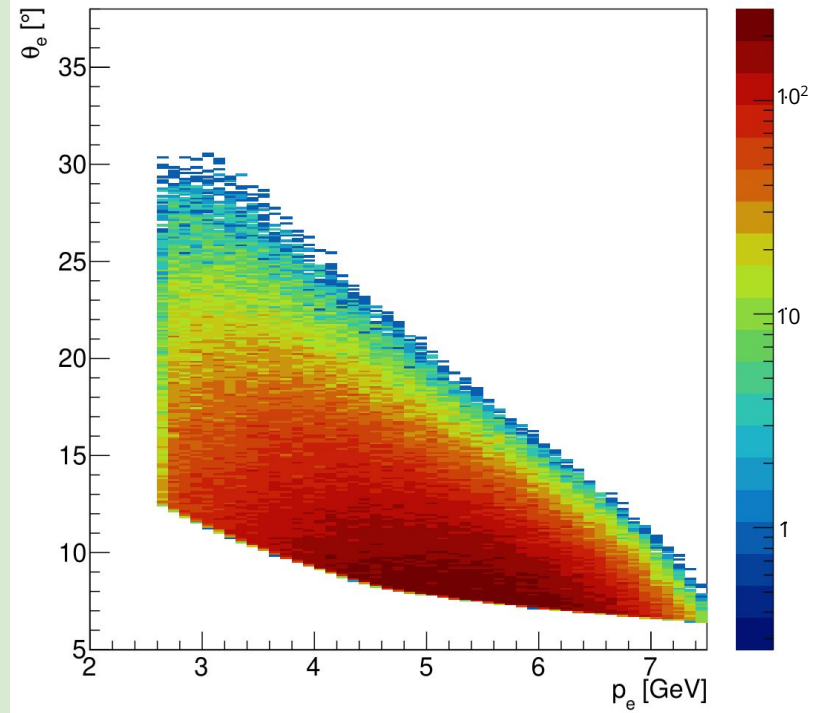
Inbending data

Electron polar angle vs momentum



Outbending data

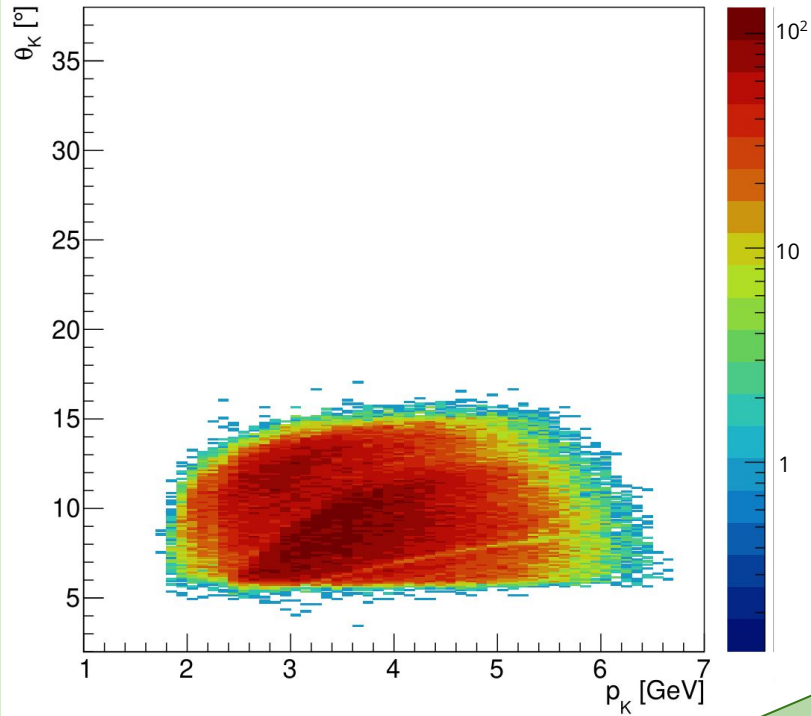
Electron polar angle vs momentum



# Phase space - hadron

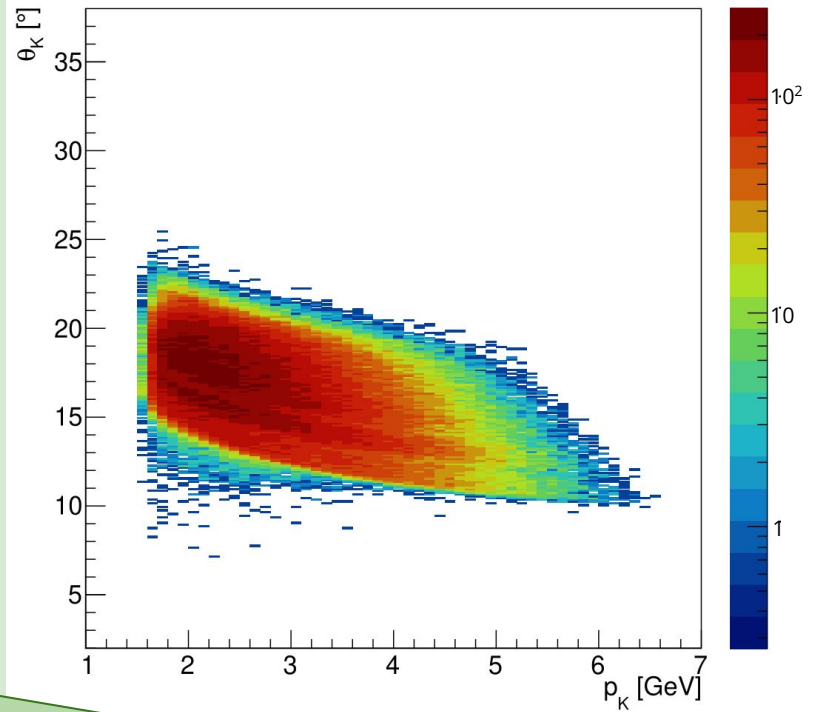
Inbending data

Hadron polar angle vs momentum



Outbending data

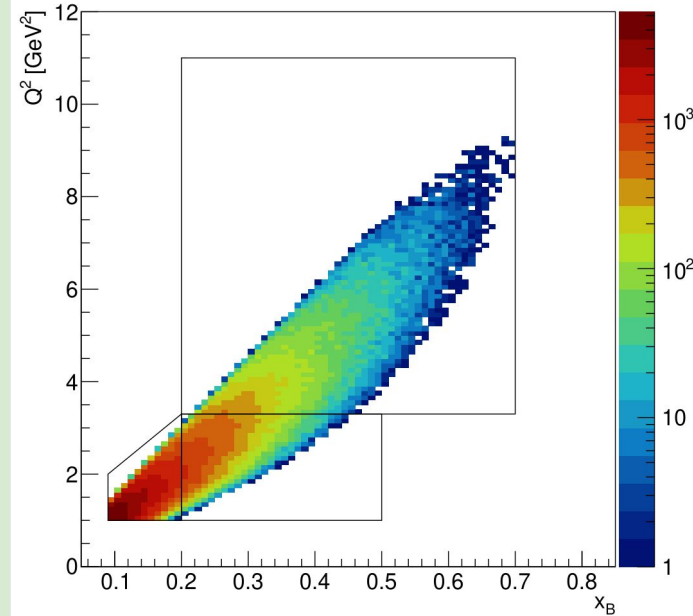
Hadron polar angle vs momentum



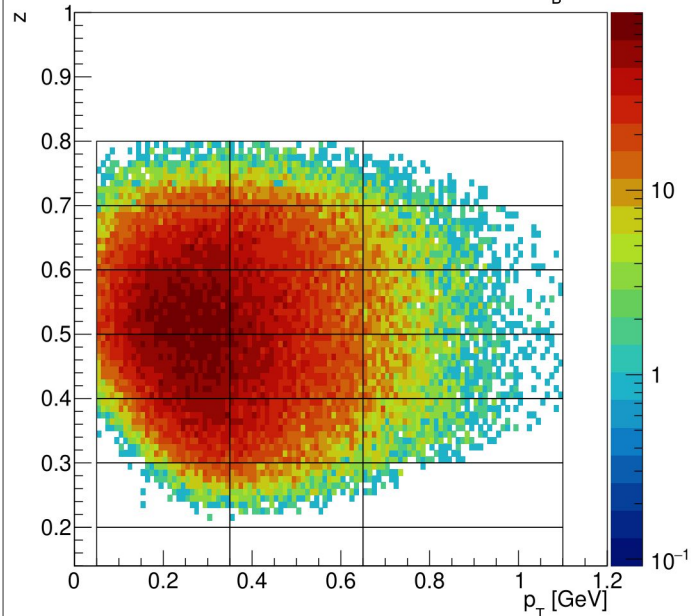
RICH acceptance in polar angle is still limited to forward particles, it could grow up to  $26^\circ$ .

# 4 dimensional binning

$Q^2 x_B$  distribution



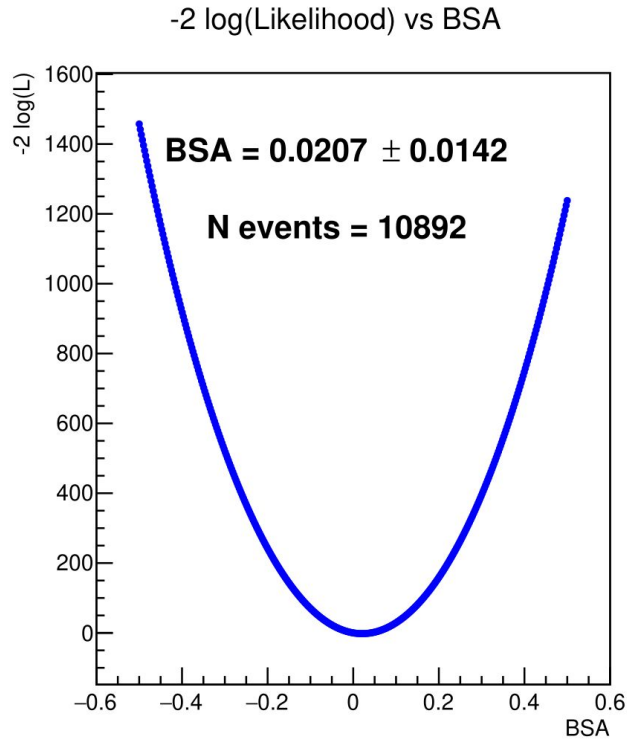
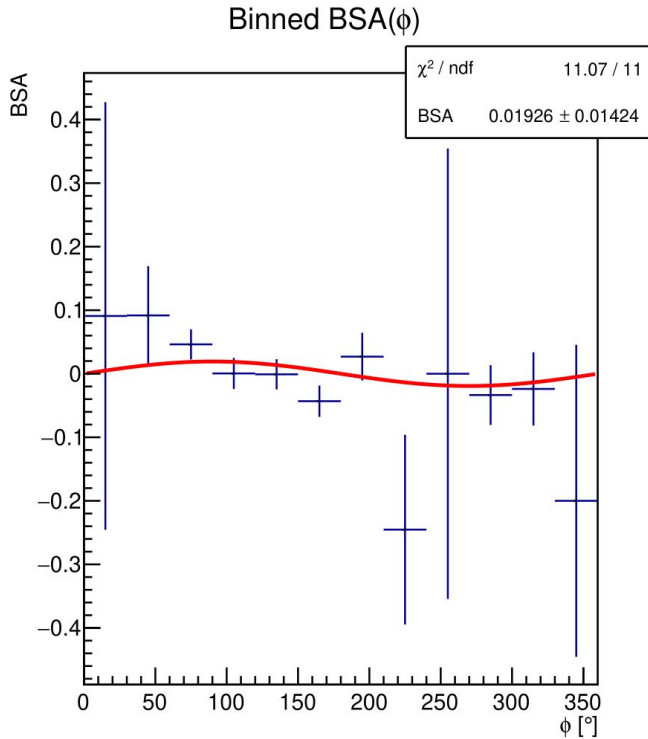
$z$  vs  $p_T$  distribution for bin  $_{Q^2, x_B} 2$



For each of the 3 bins in  $Q^2 x_B$ :

- 3 bins in  $p_T$  and BSA extracted as a function of  $z$ ;
- 3 bins in  $z$  and BSA extracted as a function of  $p_T$ .

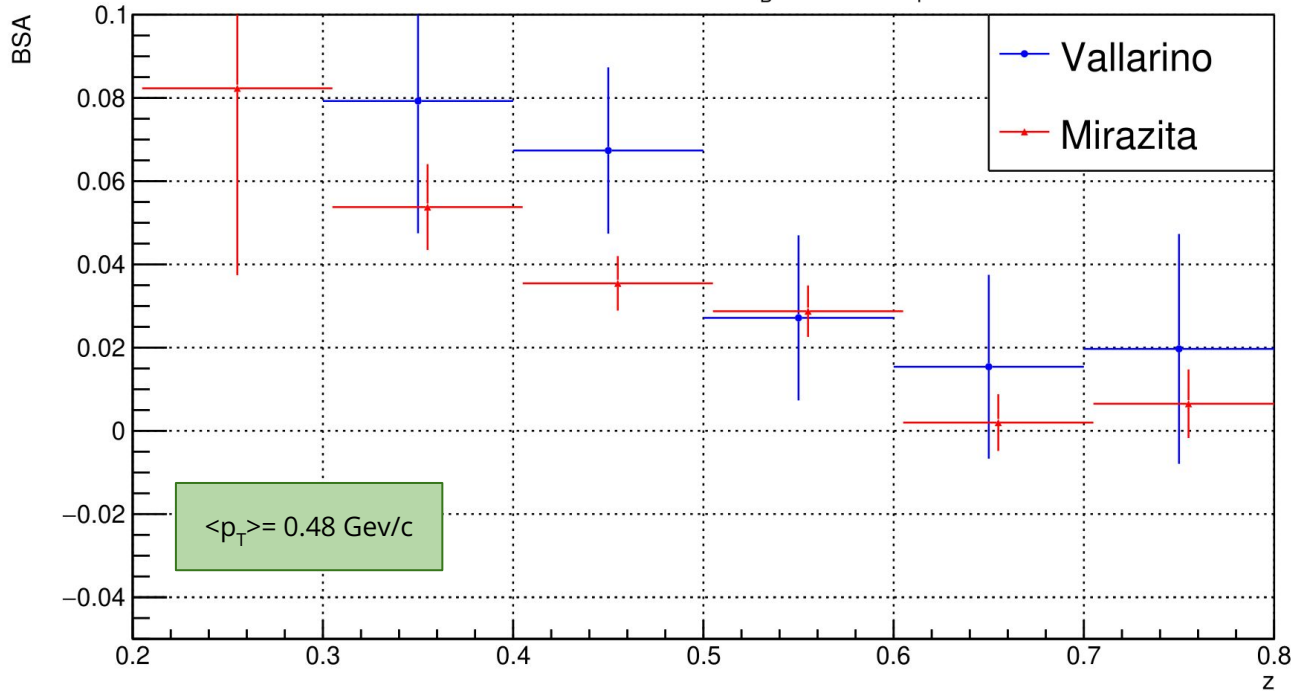
# Analysis validation - comparison of UML and binned fit



Results provided by the binned method and the UML are comparable with a similar statistical error.

# Analysis validation - status

BSA vs  $z$  - bin <sub>$Q^2 \times_B$</sub>  0 - bin <sub>$p_T$</sub>  1



Comparison of the BSA extracted using my UML fit and Mirazita results.

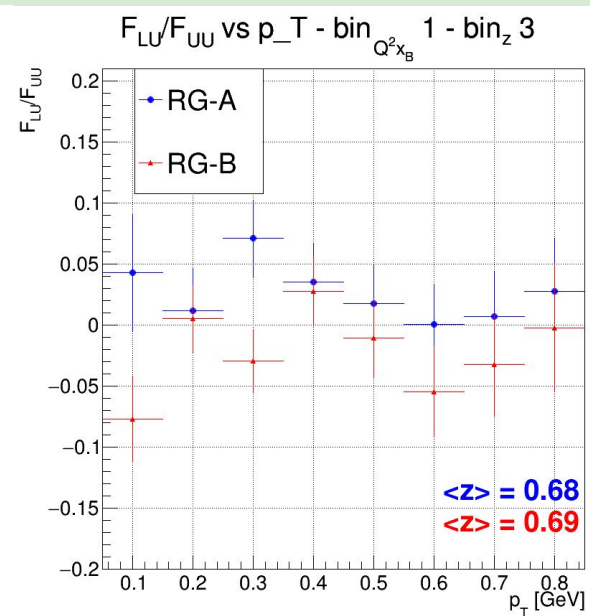
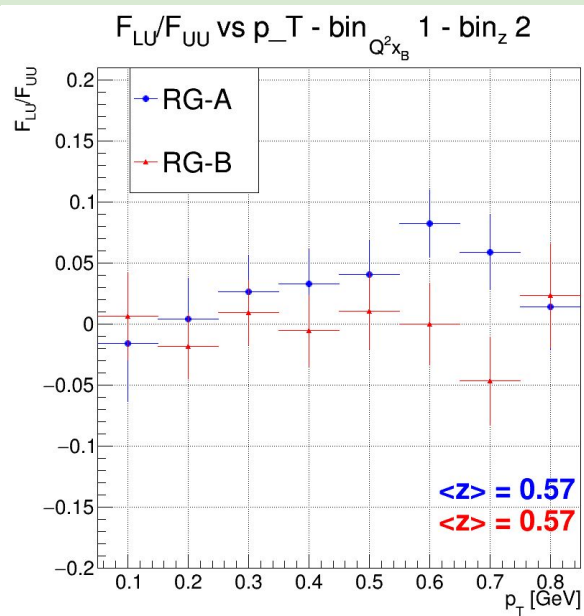
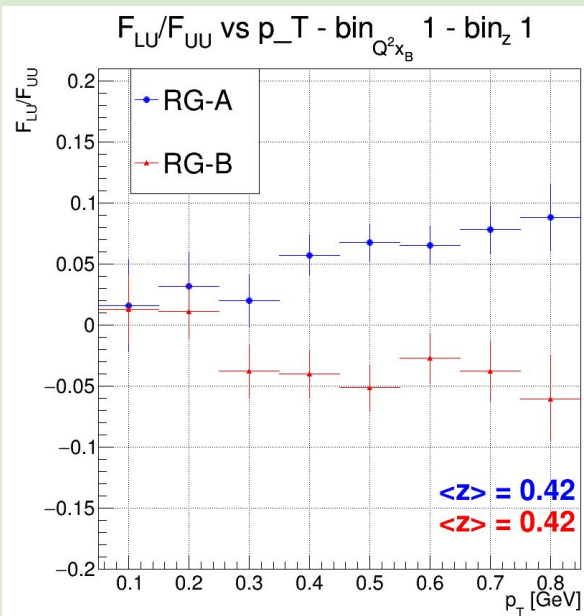
Currently, my selection removes almost  $\frac{1}{3}$  of data more than Mirazita analysis  $\rightarrow$  the issue is under investigation.

The difference in statistics is not enough to explain the difference in error bars.

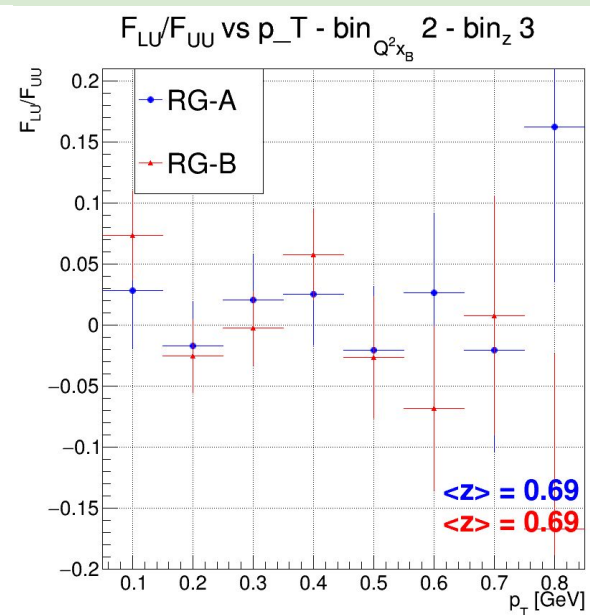
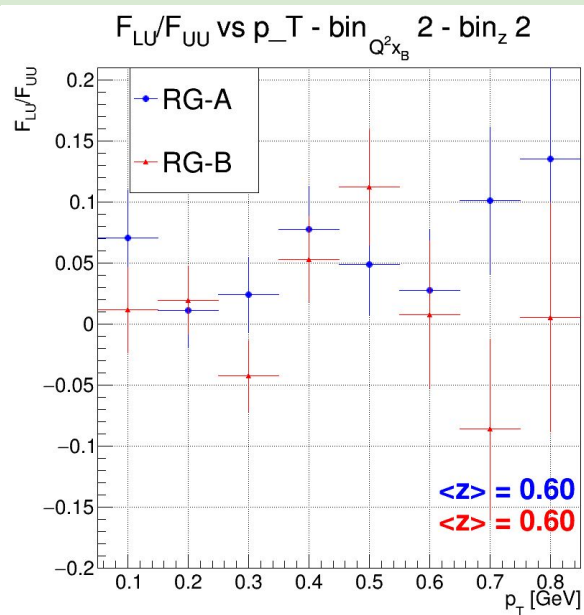
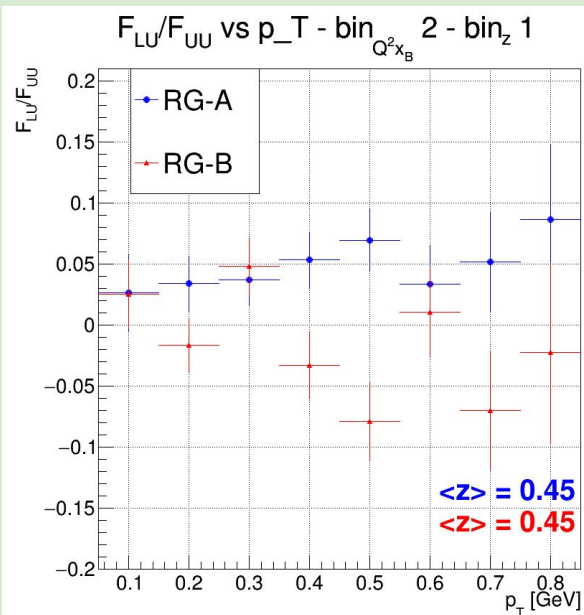
# RGB preliminary observation



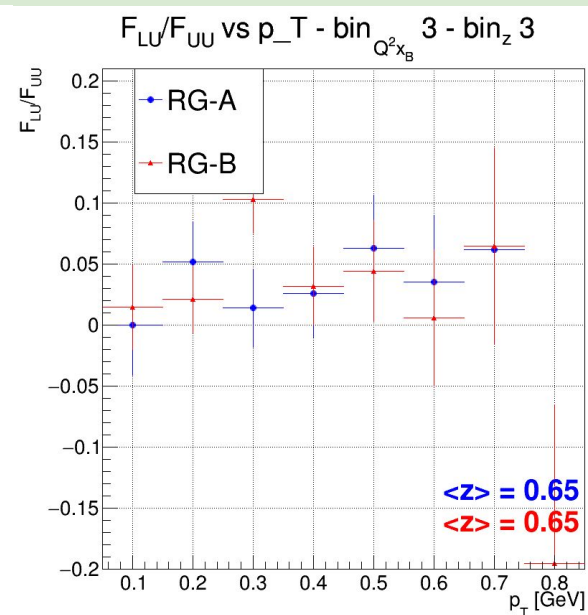
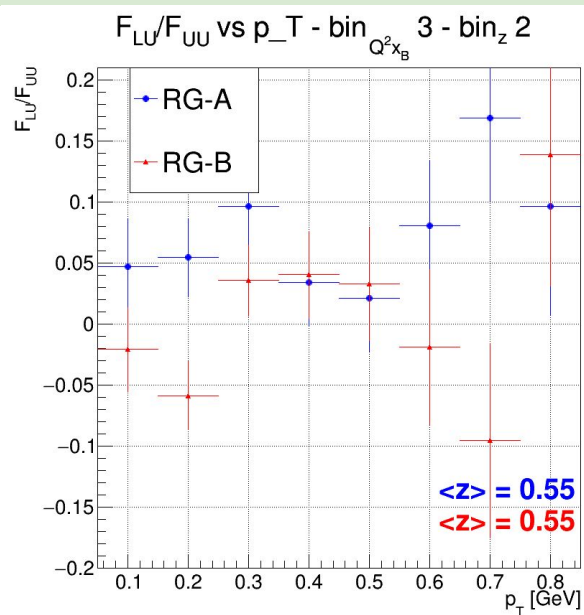
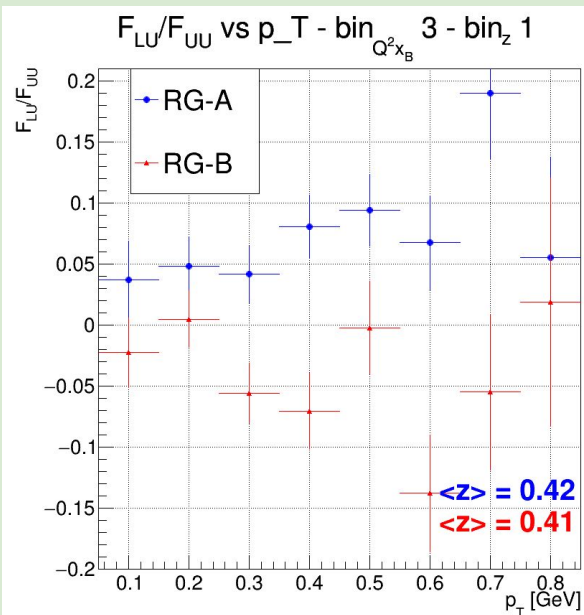
# RG-B preliminary observation



# RG-B preliminary observation



# RG-B preliminary observation



# Outlook

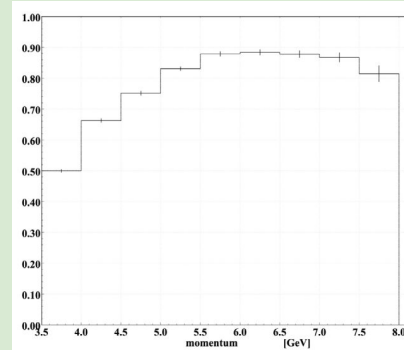
- To check my selection code to find the origin of the huge statistical error;
- To complete the analysis validation by obtaining the results provided by M. Mirazita and A. Kripko;
- To apply the validated code to the RG-B data, checking the preliminary observation reported here;
- To compare the new results with simulation and complete the analysis.

# Backup slides

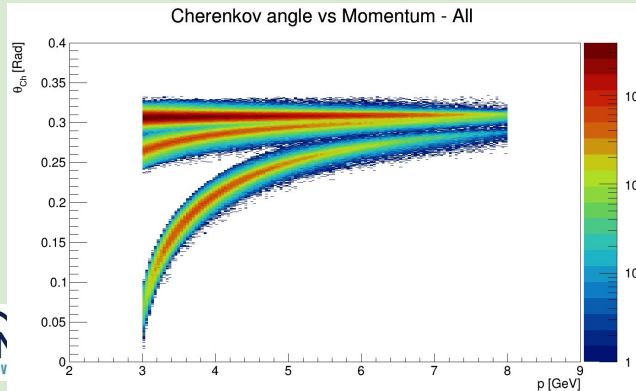
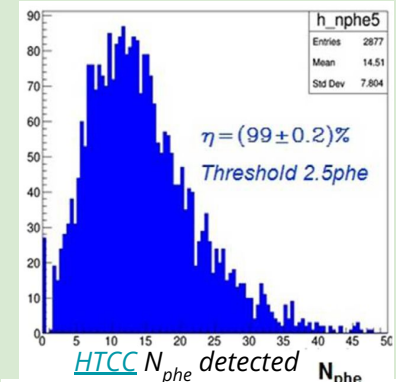
# Identify kaon at CLAS12

The CLAS12 PID is based on

- High Threshold Cherenkov Counter (HTCC): to distinguish electrons and positrons from hadrons up to 4.5 GeV/c;
- Low Threshold Cherenkov Counter (LTCC): to tag pions between 3.5 and 8.5 GeV/c;
- Forward Time-Of-Flight (FTOF): 4  $\sigma$  separation for charged  $\pi$ /K up to 2.8 GeV/c, K/p up to 4.8 GeV/c and  $\pi$ /p up to 5.4 GeV/c.
- Ring Imaging Cherenkov (RICH) 4  $\sigma$  separation for charged hadrons between 3 and 8 GeV/c.

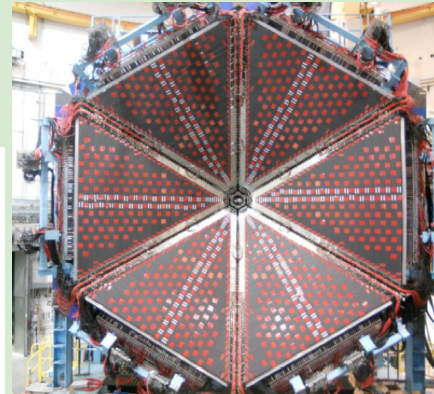


LTCC efficiency vs momentum

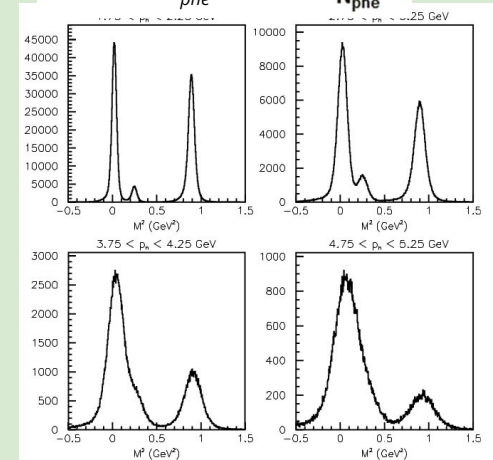


Cherenkov angle vs Momentum - All

RICH Cherenkov angle vs momentum



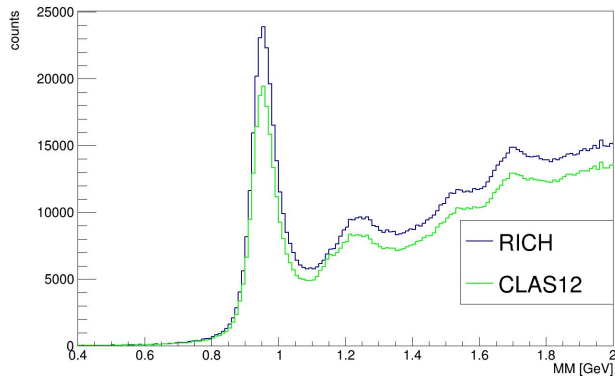
CLAS12 Forward Time-of-Flight



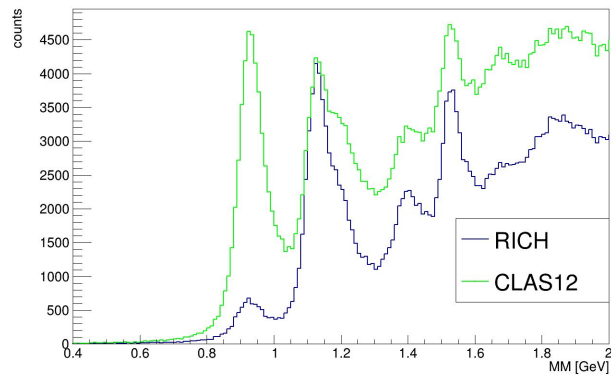
FTOF reconstructed mass square

# RICH efficiency study

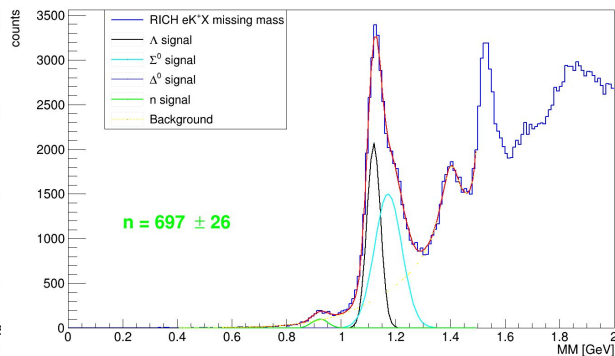
Missing mass  $e\pi^+X$



Missing mass  $eK^+X$



RICH  $eK^+X$  missing mass



The missing mass of the final state  $eH^+X$  was used to evaluate the efficiency, focusing on the neutron peak at 0.94 GeV:

- $e\pi^+n$  is an allowed exclusive process;
- $eK^+n$  is a forbidden exclusive process;

To estimate the number of neutrons  $\rightarrow$  Fit function:  $\sum_i \text{Peak}_i + \text{bkg}$ .

A quality cut was defined using the variable RQ:

- $RQ \rightarrow 0$ , identification is uncertain;
- $RQ \rightarrow 1$ , identification more reliable.

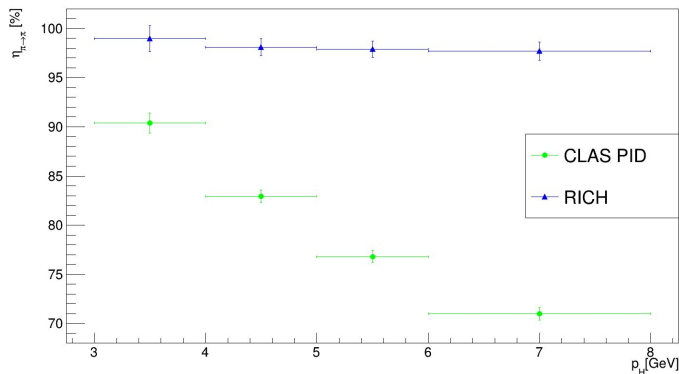
$$RQ = 1 - \frac{\lambda_{best}}{\lambda_{second\_best}}$$

To have a misidentification lower than 1% the condition is  $RQ > 0.1$

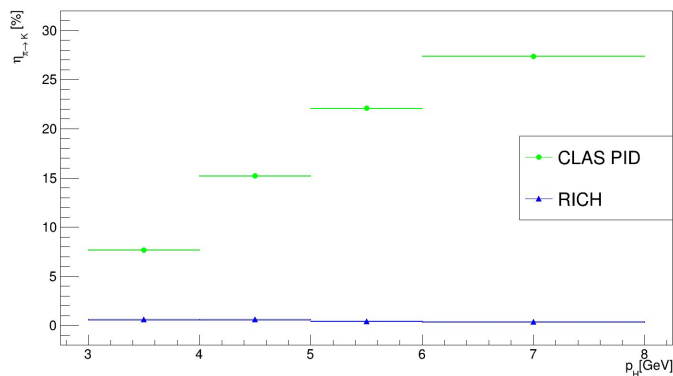
Final state	RQ cut	Number of neutrons
$e\pi^+X$	No	$186943 \pm 432$
	Yes	$171049 \pm 414$
$eK^+X$	No	$3970 \pm 63$
	Yes	$697 \pm 26$
$epX$	No	$3593 \pm 60$
	Yes	$3001 \pm 55$
Total	No	$194506 \pm 441$
	Yes	$174747 \pm 418$

# RICH efficiency results

Pion correctly identified



Pion misidentified as a kaon



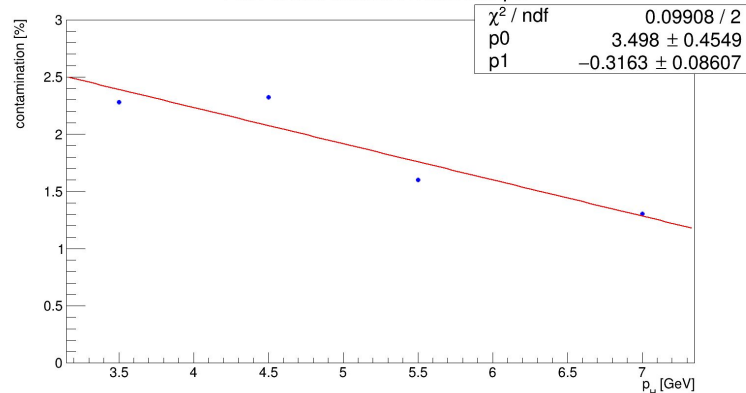
$$\eta_{\pi \rightarrow \pi} = \frac{\text{Number of exclusive neutrons in } e\pi^+X \text{ events}}{\text{Number of exclusive neutrons in } (e\pi^+X + eK^+X + epX) \text{ events}}$$

$$\eta_{\pi \rightarrow K} = \frac{\text{Number of exclusive neutrons in } eK^+X \text{ events}}{\text{Number of exclusive neutrons in } (e\pi^+X + eK^+X + epX) \text{ events}}$$

$$\eta_{\pi \rightarrow K}^{RICH} (3 \text{ GeV} < p_H < 8 \text{ GeV}) = (0.4 \pm 0.1)\%$$

$$\eta_{\pi \rightarrow K}^{CLAS12} (3 \text{ GeV} < p_H < 8 \text{ GeV}) = (19.6 \pm 0.6)\%$$

Pion contamination in kaon sample



It was possible to evaluate the pion contamination in the kaon sample as the product of  $\eta_{\pi \rightarrow K}$  with the ratio of numbers of pions over kaons.